Chapter 5

Fabrication, Characterization, Comparison of p-SnS/n-Si and p-SnS:Ag/n-Si Heterojunction Solar Cell

The fabrication of solar cell with low cost, less toxic, highly efficient and environmental welcoming process is the recent challenge for the researchers [233-237]. The photovoltaic devices fabricated with colloidal semiconducting nanoparticles recommend the opportunity for achieving the target. Semiconductor nanocrystals have gained great attraction due to their various novel properties which are different from their bulk counterperts and huge application in the potential field of heterojunction solar cell, quantum dot sensitized solar cell, Li-ion battery, photodector [238-240]. The constantly increasing demand for the alternative renewable energy supply has encouraged an innovative scientific research in the area of photovoltaic technology. A solar cell which is commonly known as photovoltaic (PV) cell, converts the light energy directly into electricity with the photovoltaic effect. The conversion of photon energy into utilizable form of energy is the basic idea of the solar cell. The term solar cell is defined as devices which absorb energy from sunlight specifically, whereas the term photovoltaic cell is exploited when the source of light is unspecified. However, the term light is employed as the electromagnetic energy produces by the Sun on the earth surface. Photovoltaic technology is the main field of science and research interconnected with the application of solar cells to produce current electricity from the solar energy. Solar energy possesses one mainly significant application because of the growing demand of fossil fuels. Therefore, the solar energy can be considered as alternative green, abundant, and renewable energy sources to fill up the deficiencies of energy. The effects of quantum confinement, aspect ratio of the nanocrystals have altered the various properties

(structural, morphology, optical and electronic) of the nanocrystals from their bulk structure. Tin sulfide (SnS) is a significant and promising semiconducting material in the field of optoelectronic devices technology such as thin film solar cell, DSSC, Li-ion batteries, photo detectors, NIR photo detectors etc. SnS has a bulk band gap of 1.3 eV [45].

The working principle of the heterojunction solar cell is based on the absorption of photons and production of charge carriers within the junction. These carriers should be separated and reach the respective electrodes without any recombination. Reported results showed that to increase the efficiency of the solar cell, a high quality of SnS layer is required. This is done either by using a good absorber active layer material or by increasing the thickness of active layer [241]. But the thickness of the active layer is restricted by the carrier diffusion length. Hence the thickness of the layer must be less than the carrier diffusion length. If the width of the active layer material is greater than the carrier diffusion length then the charge carriers would recombine before reaches to the electrodes. As a result there is decrease in current in the external circuit and hence reduce the activity of the solar cell [241]. In this chapter we have prepared SnS and SnS-Ag nanocomposite to fabricate heterojunction solar cell by cost effective method. We have also discussed how plasmonic nanoparticles influence the photovoltaic properties of the semiconducting nanoparticles. The tin and sulfur are available large in nature, non toxic and cost effective. Therefore, we have fabricated low cost, non toxic as well as more efficient SnS based heterojunction solar cell compared to other solar cell devices in which the constituent elements are more expensive, toxic and also limited in nature.

SnS and SnS-Ag nanocomposite were synthesized by cost effective solvothermal technique. Structural properties were characterized by X-ray diffraction (XRD), Transmission Electron Microscopy (TEM) and Field Emission Scanning Electron Microscopy (FESEM). Elemental compositions were confirmed by Electron Diffraction X-ray Analysis (EDAX).

Optical properties were characterized by UV-VIS absorption spectra, Photoluminescence spectra (PL) and Time Correlated Single Photon Counting (TCSPC). The solar cells consisting of heterostructure of n-Si/p-SnS/Al and n-Si/ p-SnS: Ag/Al was fabricated. SnS and SnS-Ag nanoparticles are coated on n-Si wafer to fabricate heterojunction solar cell. Our aim is to grow cost effective heterojunction solar cells with good efficiency. J–V characteristics of the fabricated SnS/Si and SnS: Ag/Si heterojunction solar cells have been studied under dark as well as under illumination. Open circuit voltage (V_{oc}), Short circuit current (J_{sc}), fill factor (FF) as well as efficiency (η) were determined.

5.1. Experimental section

SnS nanoparticles and SnS: Ag nanocomposite has been prepared by simple cost effective solvothermal method. Tin chloride ($SnCl_2.2H_2O$), Sodium sulfide ($Na_2S.XH_2O$), Polyvinyl pyrrolidone (PVP), Silver nitrate ($AgNO_3$), Ethylene glycol (EG) were used to prepare SnS nanoparticles and SnS:Ag nanocomposite. The method of sample preparation and its structural, optical characterization have been discussed in chapter 3.

5.1.1. Fabrication of photovoltaic device

In this study the solar cells consisting of hetero structure of n-Si/p-SnS/Al and n-Si/ p-SnS: Ag/Al were fabricated in the following manner. Before the fabrication of device, n-Si wafers were cleaned by ultrasonification using washing powder, deionized water and ethanol sequentially. Finally, Si wafers were etched in 1 % dilute hydrofluoric acid (HF) solution. Thin layer of SnS and SnS: Ag dispersed in ethanol was spin coated on the Si wafer rotating with a constant speed (1500 rpm for 30 s) by a spin coater. Homogeneous layers of SnS nanofilm are coated on one n-Si wafer and SnS: Ag nanofilm is coated on another n-Si wafer. The thicknesses of the layers were calculated by Surfometer. After that, the devices were annealed at 50 ^{0}C for few minutes. Al dot was deposited on SnS and SnS-Ag nanofilm by vacuum evaporation with a contact of radius 0.1 mm. Hence the contact area is 3.14×10^{-4}

cm^2. A Xe lamp (LUXTEL) with output power of 3 mW was used as an illumination source. So the intensity or power density of the incident radiation will close to 9.5W/cm^2. Finally the J-V characteristics of the fabricated devices both in dark and under light (9.5W/cm^2) were measured using a Keithley nanovoltmeter 2182a, source meter 2400, and 6221 ac/dc current source meter interface with LabVIEW program.

5.1.2. Electrical contact fabrication

Stainless-steel metal mask have been fabricated through electrochemical fabrication process. The thickness of stainless-steel metal sheet was 40 μm. The pattern design contains a hole arrangement of circles 150 μm in diameter with a pitch of 400 μm which covers 35 × 35 mm^2 substrate area. Finally, high purity Al dot was deposited on the surfaces of SnS and SnS-Ag nanofilm by vacuum evaporation hrough stainless-steel metal mask. The contact radius of Al dot was measured and it was found to be 0.1 mm. Therefore the contact area is 3.14×10^{-4} cm^2.

5.2. Plasmonic mechanisms

Plasma loading is an effective strategy to improve sample performance when the semiconductors nanoparticles are decorated with plasmonic (metal NPs) nanoparticles. These plasmonic NPs can increase the absorption ability of the semiconductor nanoparticles (with small absorption coefficients) by trapping the light into the semiconductor [242-243].Besides, plasmonic or metal nanoparticles can absorb the entire visible light spectrum with smaller energies than the band gap of semiconductor nanoparticles and consequently transfer the absorbed energy into the semiconductor NPs. The electrons which have greater energies than the Fermi level of metal is called “hot electrons” [244]. At this time, the plasmonic nanoparticles can extensively improve the different properties of semiconductors NPs such as structural, optical, electrical and optoelectronic properties. The enhancement of the optical absorption of the semiconducting nanoparticles in the presence of metal nanoparticles is the

basic mechanism of plasmonic NPs. The illumination in the optical region can encourage a collective oscillation to the valence electrons of metal NPs [245]. This is called localized surface plasmon resonance (LSPR). The oscillating cloud of electrons which are called localized surface Plasmon shows a life-time in the order of femtoseconds. But, this life time is restricted by different radiative and non-radiative decay processes [246]. In the radiative decay process the population of surface Plasmon is converted into photons, while, in case of non-radiative decay process the population is converted into electron (e) – hole (h) pairs by interband and intraband transition (Fig. 5.1). Novel metal nanoparticles whose surface plasmons generally decay by non-radiative damping processes are labelled as light absorbing NPs. As the solar energy is trapped by the NPs and consequently transferred to the atmosphere in the form of heat energy. When metal NPs is embedded with a semiconductor NPs the surface energy of Plasmon can be taken for both radiative as well as non-radiative damping. The surface energy of Plasmon transferred from the Plasmonic NP to the semiconductor and then converted to electrical energy. The transfer of energy is likely through four different mechanisms which are (a) light scattering or radiative decay (b) hot electron injection (HEI) or non-radiative decay (iii) light concentration (iv)Plasmon induced resonance energy transfer (PIRET). Light scattering through radiative decay increases the effective span of optical path within the semiconductor NPs, consequently increased the absorption and generate huge numbers of charge carriers [247]. In non-radiative decay the hot electrons of metal NPs transferred to the conduction band (CB) of the semiconductor NPs and hence the separation of hot electron (e) and hole (h) pairs. In the third and fourth mechanisms, the enhancement of localized electric field near the plasmonic NP encourages interband transition in a nearest semiconductor NPs. In last two mechanisms, the plasmon surface energy transfer to the semiconductor NPs is conciliated by coupling between photons, plasmons and excitons in the near-field of plasmonic NPs [247].

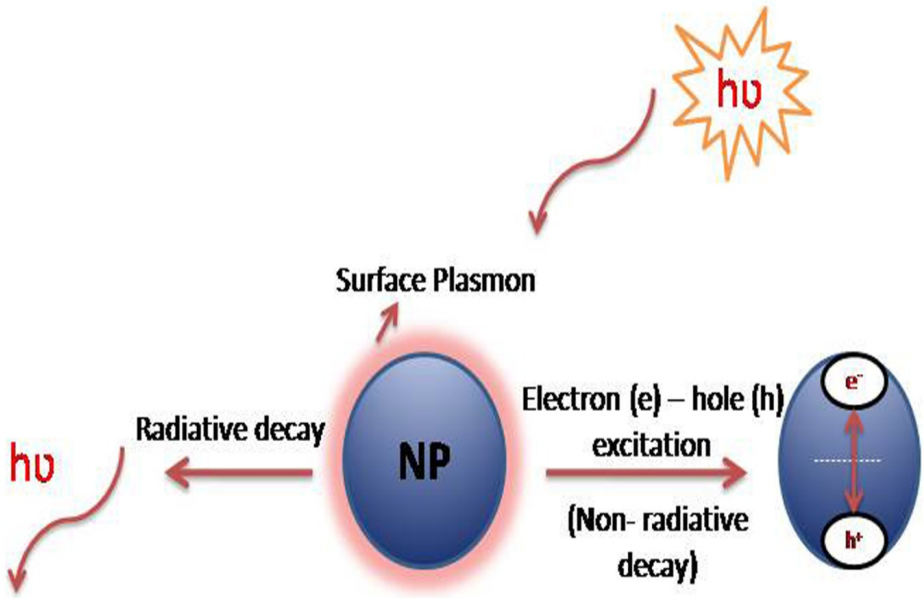

Fig. 5.1. Illustration of the NP surface Plasmon mechanism.

5.3. Results and discussion

5.3.1. Performance of solar cells

The energy band diagram of p-SnS/n-Si is shown in fig. 5.2. When visible radiation is incident on p-SnS and p-SnS-Ag, the electrons (which are minority carriers) are generated on p-SnS and p-SnS-Ag due to transition of electrons from valence band to conduction band. The electrons experience an electric field at the junction and gives rise to photocurrent. The electrical behaviour of the photovoltaic cells of pure SnS and SnS-Ag nanocomposite were analysed in the dark as well as in visible light under forward and reversed bias conditions.

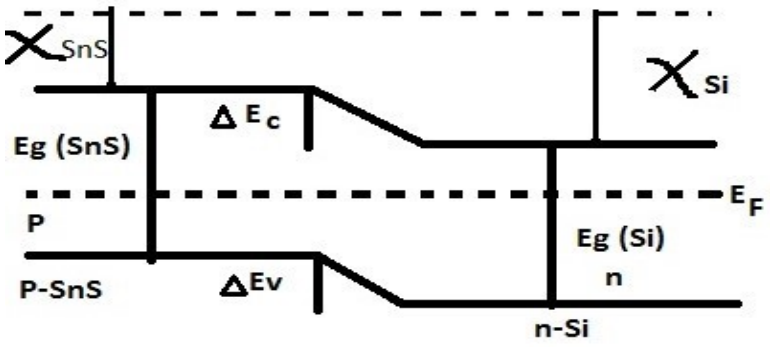

Fig. 5.2. Energy band diagram of the fabricated heterojunction

A schematic diagram of SnS based heterojunction solar cell is depicted in fig. 5.3(a,b).

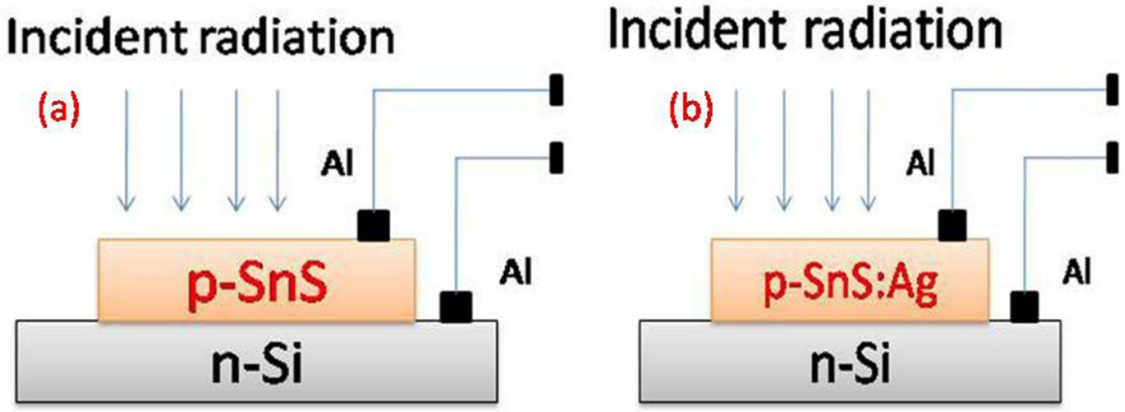

Fig.5.3. Schematic diagram of (a) SnS (b) SnS-Ag based solar cell.

Fig. 5.4(a) gives the J-V characteristics of the photovoltaic cells of SnS and SnS-Ag nanocomposite. These J-V data has been taken both in dark and illumination (9.5W/cm^2) condition under forward and reversed bias voltage in the range between -2 volt to +2 volt. The current (J) vs. voltage (V) behaviour of the photovoltaic cells under illumination is one of the most important optoelectronic characteristic for heterojunction. A small shift in SnS and a large shift in SnS-Ag nanocomposite have been observed in the J–V characteristics graph in forward bias condition under illumination with respect to the dark condition. From J-V characteristics curve different solar cell parameters like short circuit current density (J_{sc}), open-circuit voltage (V_{oc}) and maximum output power density (P_{max}) were calculated. The fabricated heterojunction solar cell device shows the behaviour just like a conventional rectifying p-n junction diode. The power density graphs (P vs V) of the p-SnS/n-Si and p-SnS-Ag/n-Si devices are depicted in fig. 5.4 (b). Fill factor (FF) and efficiency (η) of the fabricated solar cells were determined by the following relations

$$FF = \frac{V_{mp}J_{mp}}{V_{oc}J_{sc}} \qquad (5.1)$$

$$\text{and} \quad \eta = \frac{V_{oc}J_{sc}}{P_{in}}FF \qquad (5.2)$$

Where V_{oc} is the open circuit voltage and J_{sc} is the short circuit current, FF is the fill factor and η is the efficiency, P_{in} is the incident radiation power density, J_{mp} is the current at the maximum power point and V_{mp} is the voltage at the maximum power point.

The power conversion efficiency of p-SnS/n-Si and p-SnS: Ag/n-Si is 1.26% and 1.85% respectively. From the experimental results we see that the efficiency of SnS-Ag/Si heterojunction is greater than the SnS/Si heterojunction. The increase in conversion efficiency is due to the scattering effect from silver (Ag) nanoparticles [241]. Huge number of metal nanoparticles gives the result of large number of scattering. This scattering effect increase the optical path length of the incident radiation within the cells which gives rise to increase of more and more number of charge carriers and hence increase its efficiency. Thus Surface Plasmon Resonance (as evident from the absorption curve) occurring in SnS-Ag nanocomposite is responsible for greater absorption and greater efficiency compared to SnS/Si heterojunction solar cell.

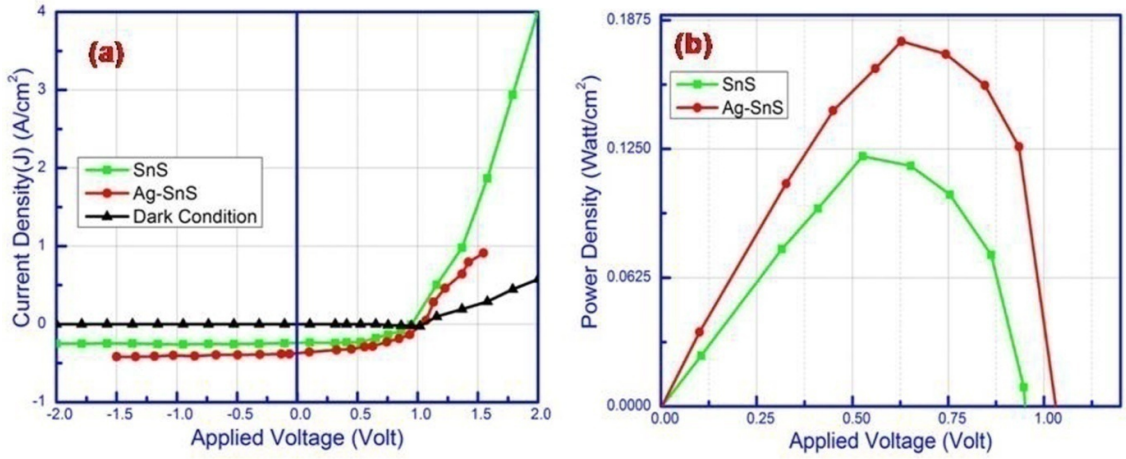

Fig. 5.4. (a) J-V characteristics of SnS/Si and SnS:Ag/Si heterojunction; (b) Variation of power density with applied voltage of SnS/Si and SnS:Ag/Si heterojunction.

The relationship between current (I) and voltage (V) of a junction diode is given by

$$I = I_0 [\exp(qV/nkT) - 1] \qquad (5.3)$$

Where, I_0 is the reverse saturation current, V is the applied voltage across the semiconductor, n is the ideality factor, k is the Boltzmann constant and T is the absolute temperature in Kelvin. The reverse saturation current has been estimated from a plot of ln (I) vs applied voltage (V) and is depicted in fig. 5.5a. The value of reverse saturation current (I_0) is achieved from the intercept of the linear region (ln (I) vs V curve) which is extrapolated to current axis. The reverse saturation current of the fabricated SnS/Si as well as SnS:Ag/Si heterojunction under dark condition is 0.695×10^{-6} A and under illumination condition are 10.95×10^{-6} A and 5.786×10^{-6} A respectively.

Taking into consideration, the junction diode equation can be expressed as [248]

$$I = I_0 [\exp (q(V - IR_s)/nkT) - 1] \qquad (5.4)$$

If we differentiate the above equation then we can write [248]

$$\frac{dV}{d(\ln I)} = IR_s + \frac{nKT}{q} \qquad (5.5)$$

Where, R_s is the series resistance of the heterojunction. The plot connected with $\frac{dV}{d(\ln I)}$ versus I gives a straight line (fig. 5.5b) and the value of diode ideality factor (n) is determined from the intercept of $\frac{dV}{d(\ln I)}$ axis. The series resistance (R_S) of the heterojunctions have been calculated from the slope of dV/d(ln I) vs. I according to equation (5.5). The value of ideality factor (n) of the constructed SnS/Si and SnS:Ag/Si heterojunction under dark condition is found to be 3.12 whereas under illumination condition are found to be 2.28 and 1.04 respectively. The short-circuit current density (J_{SC}) is determined from the J–V characteristics curve. The shunt resistance (R_{sh}) of the fabricated heterojunctions under dark and illumination of light were estimated from J-V curve using the following equation [249]

$$R_{Sh} = \left(\frac{dV}{dI}\right)_{I=I_{sc}} \qquad (5.6)$$

The series and shunt resistance of the fabricated heterojunction in light as well as in dark condition is found to be in the order of KΩ.

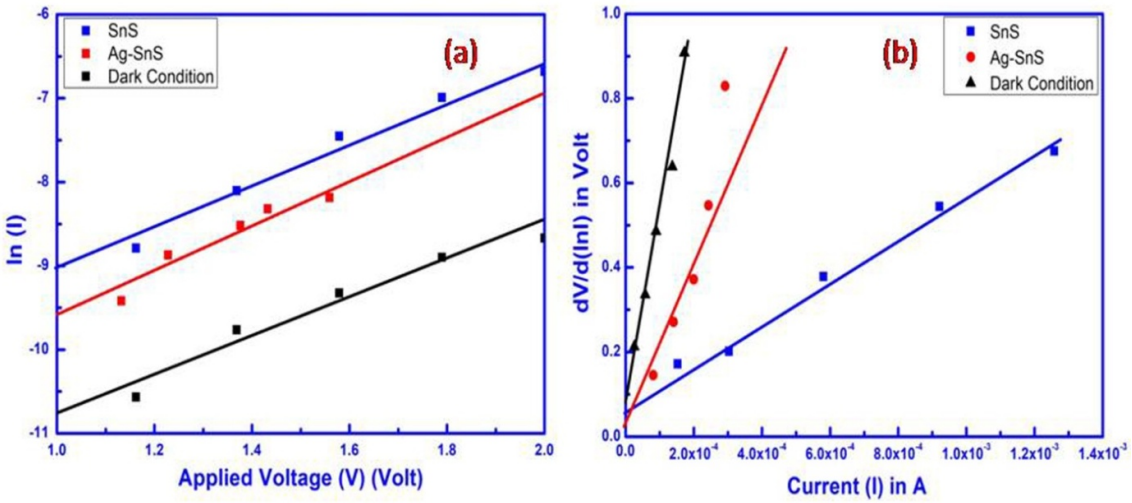

Fig. 5.5. (a) Plot of ln (I) vs V graph to determine reverse saturation current of the fabricated heterojunction; (b) Plot of dV/d(ln I) vs. I to estimate series resistance and diode ideality factor of the heterojunction.

The determined electric cell parameters of SnS/Si and SnS:Ag/Si heterojunction under dark as well as under illumination is depicted in table 5.1. The comparison of the electrical parameters with other reported work under illumination is listed in table 5.2.

Table: 5.1

Electrical cell parameters of the fabricated SnS/Si and SnS: Ag/Si heterojuncion solar cell under dark and illumination

Condition	Cell Structure	V_{oc} (V)	J_{sc} (A/cm^2)	FF (%)	η (%)	R_S (KΩ)	R_{sh} (KΩ)	n	I_0 (A)
Dark	n-Si/p-SnS/Al and n-Si/p-SnS:Ag/Al	-	-	-	-	4.39	41.02	3.12	0.695×10^{-6}
Illumination	n-Si/p-SnS/Al	0.949	0.239	52.88	1.26	0.51	26.47	2.28	10.950×10^{-6}
	n-Si/p-SnS:Ag/Al	1.021	0.377	46.0	1.85	1.83	17.75	1.04	5.786×10^{-6}

Table: 5.2

Comparison of the electrical parameters with others reported work under dark and illumination

Cell Parameters	n-Si/p-SnS/Al and n-Si/p-SnS:Ag/Al (under dark)	n-Si/p-SnS/Al (under illumination)	n-Si/p-SnS:Ag/Al (under illumination)	Referred values	References
V_{oc} (V)	-	0.949	1.021	0.523	[241]
J_{sc} (A/cm^2)	-	0.239	0.377	0.024	[250]
FF (%)	-	52.88	46.0	44.0	[251]
η (%)	-	1.26	1.85	0.35	[241]
R_S (KΩ)	4.39	2.59	1.76	5.57	[249]
R_{sh} (KΩ)	41.02	34.64	17.75	18.0	[251]
n	3.12	2.28	1.04	1.28, 1.83, 4	[249], [252]
I_0 (A)	0.695×10^{-6}	10.95×10^{-6}	5.786×10^{-6}	1.005×10^{-6}	[241]

5.4. Conclusions

SnS and SnS-Ag nanocomposite were successfully synthesized by cost effective solvothermal route. The as prepared nanoparticles are coated on n-Si wafer by spin coater to fabricate heterojunction solar cell. We have grown SnS/Si and SnS-Ag/Si heterojunction solar cell in a very cost effective way. The fabricated heterojunction demonstrates the photovoltaic behaviour. The importance of the SnS-Ag composite is evident due to the increased efficiency compared to SnS alone in the fabrication of heterojunction with Si. From J-V study of heterojunction solar cells it is evident that the power conversion efficiency of SnS-Ag/Si heterojunction is greater than the SnS/Si heterojunction. This increase in conversion efficiency of SnS-Ag/Si heterojunction is due to the scattering effect from Ag nanoparticles which leads to Surface Plasmon Resonance (SPR). Open circuit voltage and short circuit current were found to be 0.949 Volt, 0.239 A/cm^2 as well as 1.021 Volt, 0.377 A/cm^2 of SnS and SnS-Ag based heterojunction solar cell respectively. There might be further scope to increase efficiency using SnS-Ag composite with Si.